Organic & Biomolecular Chemistry

Dynamic Article Links

Cite this: *Org. Biomol. Chem.*, 2011, **9**, 8068

www.rsc.org/obc

PAPER

N-fused porphyrin with pyridinium side-arms: a new class of aromatic ligand with DNA-binding ability†

Yoshiya Ikawa,[a,b] Satoshi Touden[a] and Hiroyuki Furuta*[a,b]

Received 17th June 2011, Accepted 31st August 2011
DOI: 10.1039/c1ob05981e

N-fused porphyrin (NFP) is a porphyrin analogue with an 18π tetrapyrrolic macrocycle, in which a unique tripentacyclic ring is embedded. While the optical properties of NFP of absorbing and emitting near-infrared (NIR) light around 1000 nm are promising for its application to NIR technology, its unique structure is also attractive as a platform to construct a novel class of DNA-binding ligands. Herein, we have synthesized a water-soluble derivative of NFP (**pPyNFP**) possessing four cationic pyridinium substituents and examined its acid/base behaviors and interactions with various forms of DNAs in aqueous solution. **pPyNFP** interacts with ssDNA and dsDNA electrostatically. **pPyNFP** also interacts with a G-quadruplex DNA derived from the human telomeric sequence and causes a characteristic spectral change of the G-quadruplex DNA, which suggests that **pPyNFP** modulates the Na^+-induced (2 + 2) antiparallel G-quadruplex to the all-parallel structure.

Introduction

Porphyrins and their related pigments play pivotal roles in living cells.[1] While naturally occurring porphyrins usually form complexes with proteins, the structural features of porphyrins also make them attractive as DNA-binding ligands. Actually, porphyrins possessing pyridinium moieties, such as 5,10,15,20-tetrakis(4′-*N*-methylpyridyl)porphyrin (**TMPyP**, Chart 1) and 5,10,15,20-tetrakis(α-pyridinio-*p*-tolyl)porphyrin (**pPyP**, Chart 1), constitute a representative class of water-soluble porphyrins with DNA-binding ability.[2–4] In **TMPyP** and **pPyP**, four cationic pyridinium moieties afford not only high water-solubility but also an electrostatic affinity for the sugar–phosphate backbones of DNA. A large number of DNA-binding studies of **TMPyP**, **pPyP** and their derivatives have provided a basic framework of porphyrin–DNA interactions.[2–8] These data are not only important for biological and diagnostic applications, but are also useful for the development of new classes of DNA-binding ligands because a variety of novel platforms for DNA-binding ligands have been synthesized along with the development of porphyrin-related macrocycles (porphyrinoids).[9–13] Although DNA-binding ability has been vested to several porphyrinoids recently, the rest of them have still remained unexploited as DNA-binding ligands.[14–20]

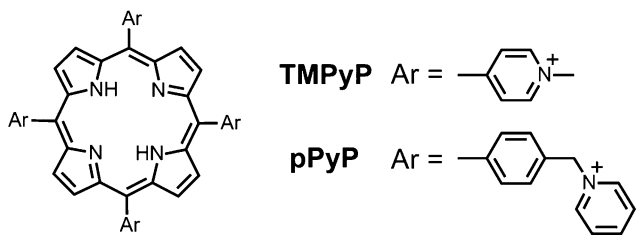

Chart 1 The structures of the cationic water-soluble *meso*-tetraaryl porphyrins possessing four pyridinium moieties.

N-fused porphyrin (NFP) is in a class of porphyrinoids with an 18π tetrapyrrolic macrocycle, in which a unique tripentacyclic ring is embedded.[21–25] Regardless of its peculiar structure, NFP can be readily prepared in two steps from a porphyrin isomer, N-confused porphyrin (NCP, Chart 2).[22,23] NFP has been attractive as a near-infrared (NIR) dye applicable to material science because of its photophysical properties of absorbing and emitting NIR light at around 1000 nm.[26] The crystal structure of N-fused tetratolylporphyrin (**NFTTP**) revealed that the tripentacyclic structure provides a unique π-plane and diminishes the steric hindrance between the aryl moiety at the C(5) position and the macrocycle.

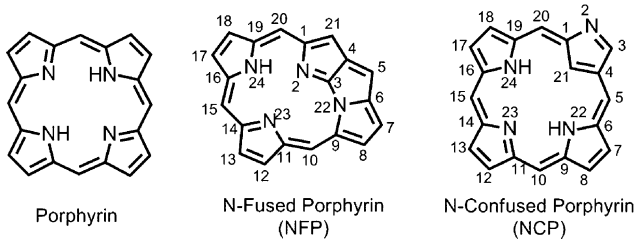

Chart 2 The basic structures of a porphyrin (left), N-fused porphyrin (middle), and N-confused porphyrin (right).

[a]*Department of Chemistry and Biochemistry, Graduate School of Engineering, Kyushu University, 744 Moto-oka, Nishi-ku, Fukuoka, 819-0395, Japan. E-mail: hfuruta@cstf.kyushu-u.ac.jp; Fax: (+81) 92-802-2865; Tel: (+81) 92-802-2865*
[b]*International Research Center for Molecular Systems, Kyushu University, 744 Moto-oka, Nishi-ku, Fukuoka, 819-0395, Japan*
† Electronic supplementary information (ESI) available: See DOI: 10.1039/c1ob05981e

The dihedral angle between the tripentacyclic ring and C(5) phenyl group (25.6°) in **NFTTP** is much smaller than that between an ordinary porphyrin plane and *meso*-phenyl group (64.3°).[22] Although these structural features of NFP are attractive as a new class of porphyrin-related DNA-binding ligand, such an ability of NFP has been totally unexploited. In this paper, the synthesis of water-soluble N-fused tetraphenylporphyrin (**NFTPP**) derivative possessing four α-pyridino-*p*-tolyl moieties (Scheme 1) and its acid/base and DNA-binding properties in aqueous solutions are described.

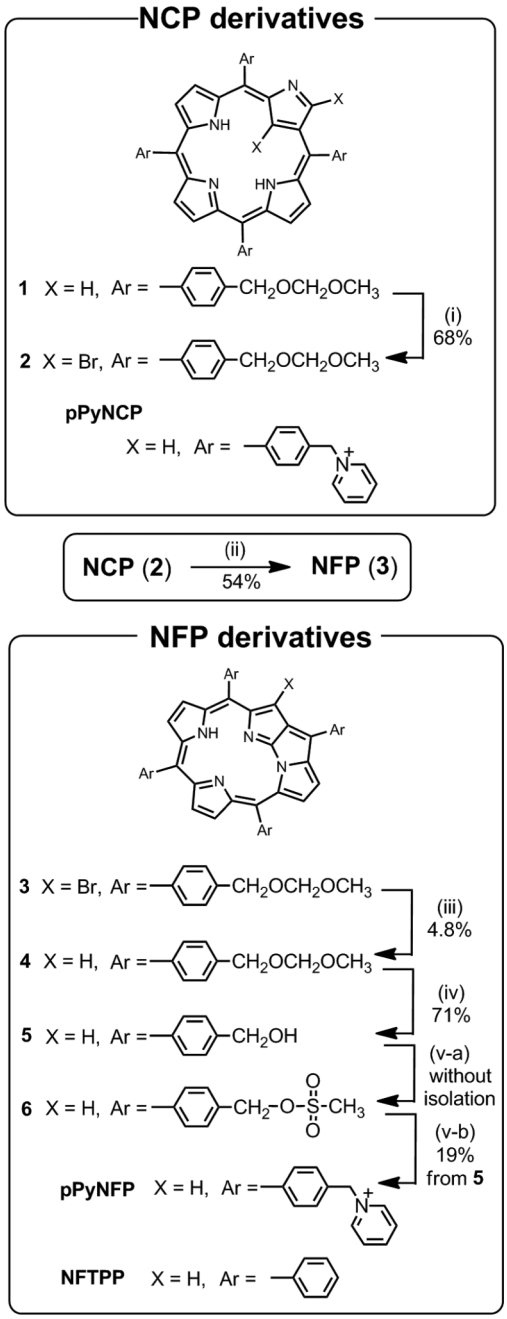

Scheme 1 The synthetic scheme of water-soluble cationic N-fused porphyrin (**pPyNFP**). The structures and chemical transformations of the NCP derivatives and NFP derivatives in this study are summarized in the top and bottom parts, respectively. The transformation of NCP (**2**) to NFP (**3**) is also shown. Reaction conditions: (i) NBS, 10 min, CH_2Cl_2; (ii) pyridine, rt, 12 h; (iii) pyridine, reflux, 12 h; (iv) TFA, H_2O, rt, 3 days; (v-a) methanesulfonyl chloride, pyridine; (v-b) pyridine, rt, 3h.

Results and discussion

Synthesis of NFP derivative with cationic side-arms

To solubilize **NFTTP** in aqueous media, we designed and synthesized N-fused tetrakis(α-pyridino-*p*-tolyl)porphyrin **pPyNFP**. The cationic α-pyridino-*p*-tolyl moiety should afford high water-solubility. The target compound (**pPyNFP**) was derived from the N-confused porphyrin (**1**) possessing four methoxymethyl (MOM) ethers (Scheme 1). At first, **1** was synthesized by an acid-catalyzed condensation of pyrrole and *p*-methoxymethoxymethylbenzaldehyde with methanesulfonic acid (MSA), followed by oxidation with 2,3-dicyano-5,6-dichloro-*p*-benzoquinone (DDQ).[12] Treatment of **1** with *N*-bromosuccinimide (NBS) afforded the dibrominated derivative (**2**), which can be readily transformed to the N-fused porphyrin derivative (**3**) by treatment with pyridine.[22,23] After removal of the bromo group at the C(21) position to yield **4**, the four MOM-ethers in **4** were converted to hydroxy groups to afford **5**. After quantitative mesylation of the hydroxy groups in **5**, the target compound (**pPyNFP**) was produced by the nucleophilic substitution of the mesylate esters in **6** with pyridine. **pPyNFP** was purified by a reverse phase HPLC with CH_3CN/H_2O containing 0.1% trifluoroacetic acid (TFA) and stored as a TFA salt. In DMF, the absorption spectrum of **pPyNFP** was nearly identical to that of **NFTPP** (Fig. 1), indicating that the α-pyridinomethylene moiety did not strongly perturb the electronic state of the **NFTPP** skeleton. The solubility of **pPyNFP** in water was confirmed by partition experiments between ultrapure water and CH_2Cl_2, in which **pPyNFP** was selectively dissolved in the water-phase (Fig. S1A†).

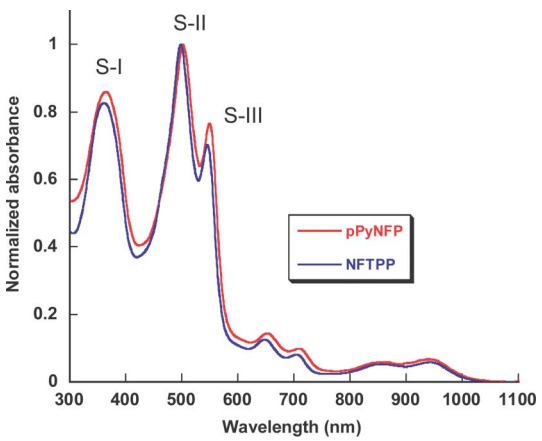

Fig. 1 UV-vis–NIR absorption spectra of **pPyNFP** and **NFTPP** in DMF.

Acid–base property of PyNFP

The acid–base property of the molecule of interest is often important for its applications in aqueous media and the cellular environment. While the acid–base properties of regular porphyrins have been studied extensively,[27–29] those of porphyrin analogues have scarcely been reported.[12,25,30] Previously, we studied the

acid–base property of a water-soluble NFP derivative (**NFP-R9**, Chart 3) possessing a phenyl substituent at C(21) position, in which the NFP skeleton underwent a two-step protonation to yield the mono- and dication in a stepwise manner.[25] The substituent at C(21), however, causes electronic perturbation on the NFP skeleton.[23] Therefore it is desirable to determine the acid–base property of the N-fused porphyrin without a C(21) substituent in aqueous solution and, for such a purpose, the structure of **pPyNFP** is suitable (Scheme 1).

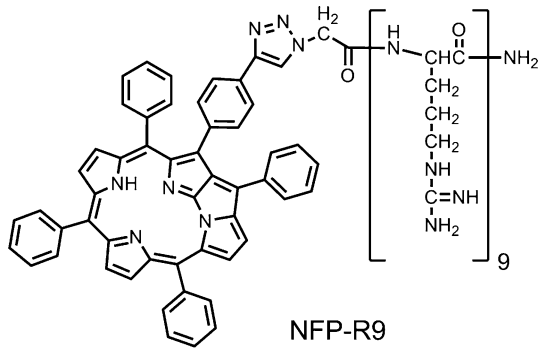

Chart 3 The structure of **NFP-R9**, a water-soluble derivative of N-fused porphyrin possessing a nona-arginine (R9) peptide tail.

The acid–base property of **pPyNFP** in aqueous solution was investigated under a wide pH range, which was adjusted with HCl (acidic region) or NaOH (basic region). Through the pH titration experiments with **pPyNFP**, we observed two pH regions in which the absorption spectra were essentially unchanged (Fig. S1†). In the pH region 8.3–11.7, the absorption spectra of **pPyNFP** (Fig. S1B†), which were similar to those of **NFTPP** and **pPyNFP** in DMF (Fig. 1), exhibit three Soret-like bands (S-I, S-II and S-III) at 359, 494 and 547 nm and Q-like bands at 649, 702, 861 and 949 nm (Fig. S1B†). In the pH region 2.2–5.0, the absorption spectra of **pPyNFP** (Fig. S1C†) were closely similar to those of the protonated form of **NFTPP** in an organic solvent. These observations clearly indicate that **pPyNFP** exists as a freebase (neutral) form at pH 8.3–11.7 and a protonated form (monocation) at pH 2.2–5.0, respectively. With a decrease in the pH from 8.3 to 5.0, a transition from the freebase to the monocation was clearly observed (Fig. 2A). In the strongly acidic region (pH <2.2), the monocation further decreased the intensity of the Soret-like bands and weakly increased the intensity at the NIR region (Fig. 2B), suggesting that the **pPyNFP** monocation accepted the second proton to form a dication. Since a similar two-step spectral change was also reported for **NFP-R9** (Chart 3),[25] the two-step protonation would be an intrinsic property of the NFP skeleton. From the titration curve, the pK_a values of each protonation process, [**2H$^+$-pPyNFP**]//[**H$^+$-pPyNFP**] and [**H$^+$-pPyNFP**]//[**pPyNFP**], were estimated to be 1.3 and 7.0, respectively. These pK_a values are comparable to those for **NFP-R9** (2.3 for [**2H$^+$-NFP-R9**]//[**H$^+$-NFP-R9**], and 6.5 for [**H$^+$-NFP-R9**]//[**NFP-R9**]).[25]

Aggregation behavior of pPyNFP

The aggregation properties of **pPyNFP** were examined in a 50 mM HEPES buffer solution because the cationic regular porphyrins, including **pPyP**, are reported to form several types of aggregates

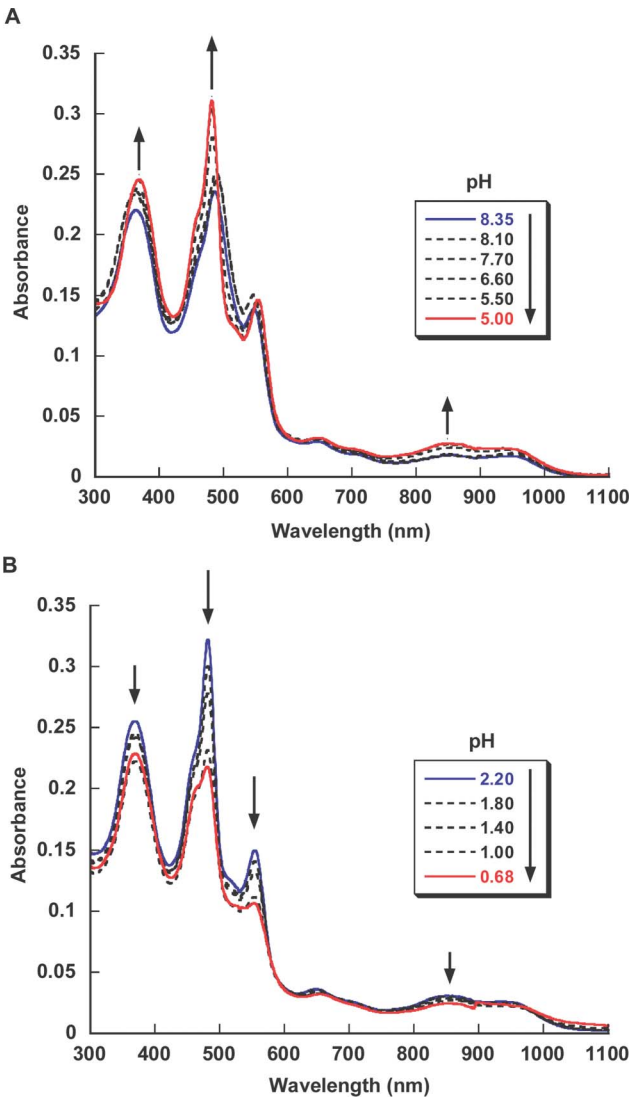

Fig. 2 The UV-vis–NIR absorption spectral changes of **pPyNFP** (7.5 μM) in H_2O titrated with NaOH and HCl. Absorption spectra for the titration at pH 8.35–5.00 (A) and pH 2.20–0.58 (B).

depending on the buffer conditions.[4,31–33] Sodium dodecyl sulfate (SDS), the critical micellar concentration of which in H_2O is 8.2 mM, has been shown to modulate the aggregation states of regular porphyrins in aqueous solution.[33] When SDS (5 mM in the final solution) was added to a buffer solution of **pPyNFP** at pH 8.5, a strong hyperchromic effect was observed without a shift of the absorption maxima (λ_{max}) (Fig. 3A). This spectral change was too large to be attributed to the small pH change (8.5 to 8.35) caused by SDS (see also Fig. S1B†). Similar SDS-induced hyperchromic effects were also observed at pH 7.0 (which changed to 6.88 by 5 mM SDS) and pH 5.0 (which changed to 5.12 by 5 mM SDS), albeit the hyperchromic effects under neutral and acidic conditions were weaker than that under basic conditions (Figs 3A and B). These results indicate that, in 50 mM HEPES buffer solutions, **pPyNFP** should assemble without any particular order because no large shift of λ_{max} characteristic of *H*- or *J*-aggregates was observed (Scheme 2). Regardless of the pH of the solution, additions of 1 mM SDS caused hypochromic changes

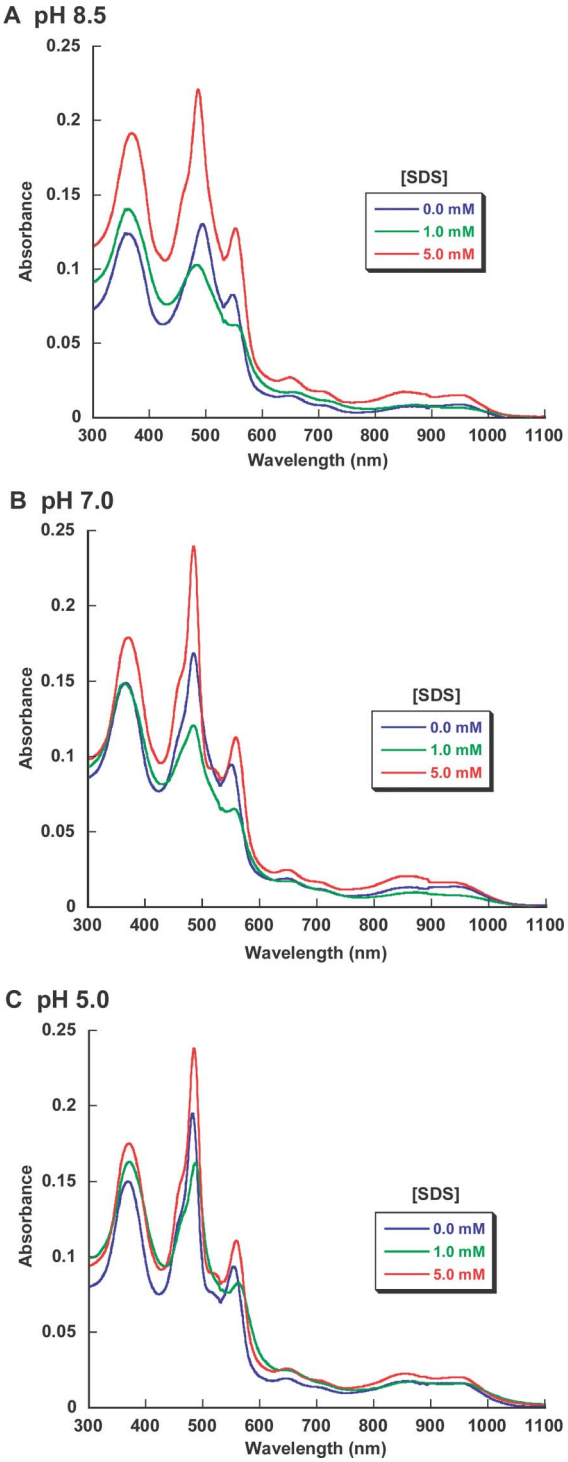

Fig. 3 The UV-vis–NIR absorption spectral changes of **pPyNFP** (7.5 μM) by the addition of various amounts of SDS at pH 8.5 (A), 7.0 (B) and 5.0 (C).

(Fig. 3). Under the 1 mM SDS conditions, **pPyNFP** and SDS presumably form hydrophobic aggregates (Scheme 2), in which the SDS concentration is sufficient to neutralize the cationic charges of the pyridinium moieties of **pPyNFP**, but too low to disperse **pPyNFP**. **pPyP** also exhibited two-step, SDS-dependent spectral changes in 50 mM HEPES buffer solutions (Fig. S2†).

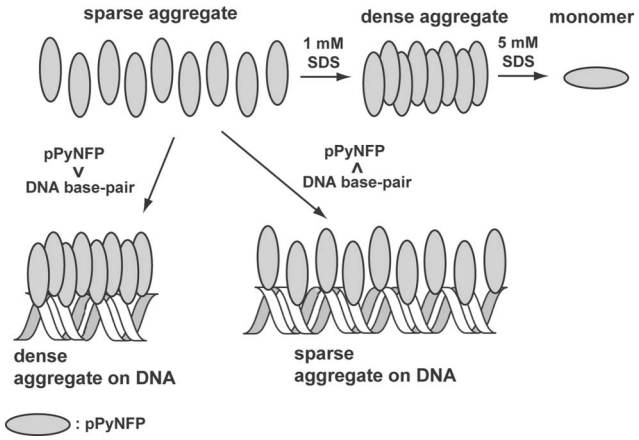

Scheme 2 Plausible aggregation/disaggregation behaviors of **pPyNFP** in the presence of different concentrations of SDS or DNA.

Interactions with double- and single-stranded DNAs

Recently DNA-binding studies of porphyrin analogues have been reported and some of them exhibited characteristic properties that were distinct from regular porphyrins.[9–12] Therefore, it is of interest to investigate the interactions between DNA and **pPyNFP**, the pyridinium side-arms of which should have the ability of electrostatic interactions with the sugar–phosphate backbones of DNA.

We first investigated the interactions to the long double-stranded DNA (dsDNA) in a pH 7.0 buffer solution, in which **pPyNFP** exists as a mixture of freebase and monocation (Fig. 2A). Upon the addition of less than an equimolar amount of DNA base pairs, **pPyNFP** exhibited a hypochromic change with a red-shift, in which S-II was shifted from 485 to 493 nm (Fig. 4A). In the presence of more than one equivalent molar amount of DNA base pairs, however, **pPyNFP** exhibited a hyperchromic spectral change without a further shift of λ_{max} (S–II was 495 nm) (Fig. 4B).[34] Such two-step changes were not observed in the regular porphyrin (**pPyP**), the spectral changes induced by dsDNA of which were unidirectional (a red-shift of the Soret band (414 to 421 nm) with hypochromic change). To investigate whether **pPyNFP** induces the structural change of dsDNA, we measured the circular dichroism (CD) spectra of dsDNA, which showed the CD signal of B-form DNA in the range 220–300 nm (Fig. 4C). Upon the addition of **pPyNFP**, the CD signal of dsDNA was diminished (Fig. 4C).

In the presence of less than an equimolar amount of dsDNA base pairs, dsDNA may act as a glue or raft, on which **pPyNFP** was condensed (Scheme 2). While this mode of association should accompany a hypochromic shift, the observed bathochromic shift (red-shift) should be caused by the interaction between the NFP macrocycle and dsDNA. In the presence of an excess molar amount of dsDNA base pairs, the dense aggregation of **pPyNFP** on dsDNA should be resolved, but the interaction between the NFP macrocycle and dsDNA should be retained (Scheme 2).

To see whether A:T and G:C base pairs cause different effects on **pPyNFP**, we examined the effects of two synthetic DNAs (5′-ATATATATATATATATATAT-3′: $d(AT)_{10}$) and 5′-GCGCGCGCGCGCGCGCGC-3′: $d(GC)_{10}$), which can form duplexes with only A:T and G:C base pairs (designated as $[d(AT)_{10}]_2$ and $[d(GC)_{10}]_2$), respectively. Upon the addition of these

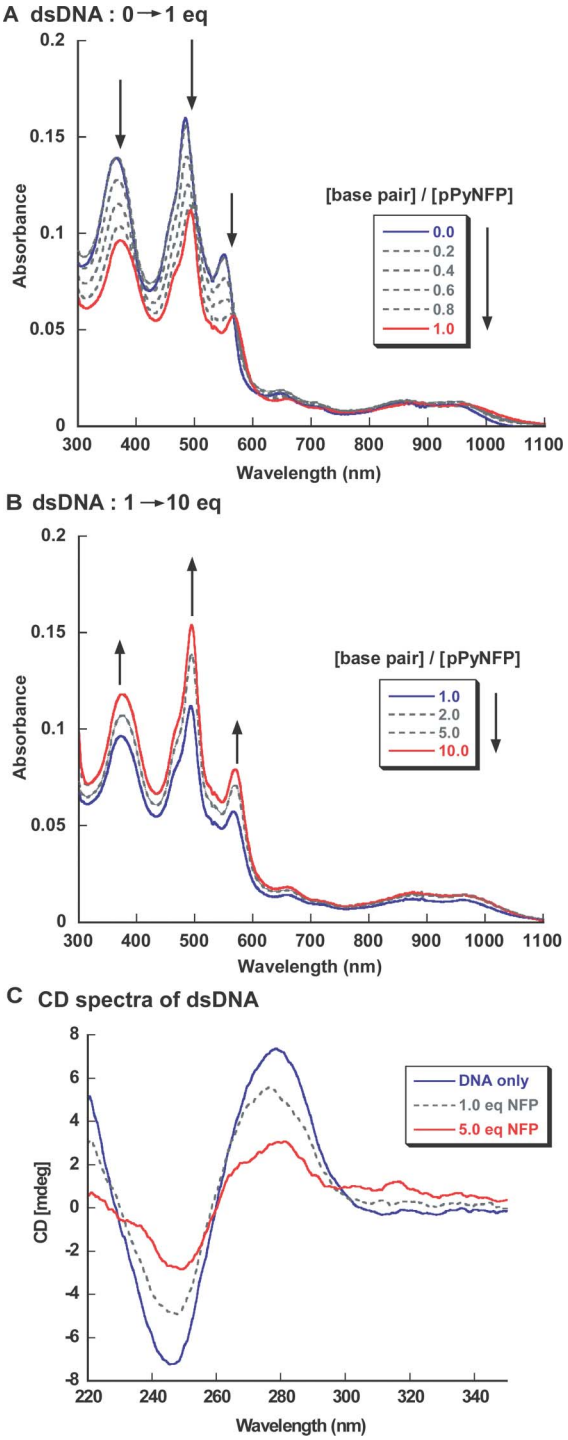

Fig. 4 The double stranded DNA (dsDNA) binding ability of **pPyNFP**. A, B: UV-vis–NIR absorption spectra of **pPyNFP** (7.5 μM) in the presence of less (A) or more (B) than 1 equivalent molar amounts of dsDNA base pairs at pH 7.0 with 50 mM HEPES. C: Circular dichroism (CD) spectra of dsDNA in the absence and presence of **pPyNFP** at pH 7.0 with 50 mM HEPES.

two DNAs, the overall patterns of the spectral changes resembled those caused by dsDNA (Figs 5A and B). On the other hand, the hypochromic change and its recovery were more remarkable with $[d(AT)_{10}]_2$ (Fig. 5A) than with $[d(GC)_{10}]_2$ (Fig. 5B). To further investigate the interactions between **pPyNFP** and $[d(AT)_{10}]_2$ and $[d(GC)_{10}]_2$, CD spectra induced in the Soret band of **pPyNFP** were measured (Figs 5C and D). In the presence of a 1.0 equimolar amount of DNA base pairs, $[d(AT)_{10}]_2$ (Fig. 5C) and $[d(GC)_{10}]_2$ (Fig. 5D) gave different CD signals. These results strongly suggest that different binding-modes are used by **pPyNFP** to associate with $[d(AT)_{10}]_2$ and $[d(GC)_{10}]_2$. In the presence of dsDNA, the induced CD spectra were similar to those in the presence of $[d(GC)_{10}]_2$ (Fig. S3†).

The effects of single-stranded DNA (ssDNA) were also examined using a 20-nucleotide oligomer (5′-TGTAGGCATGCTTAAGCAT-3′), which contains an approximately equal number of four nucleobases and, thus, is unlikely to form particular secondary structures. In the presence of less than two equivalent molar amounts of nucleobases, a hypochromic change with a slight red-shift, in which S-II was shifted from 485 to 493 nm, was observed (Fig. 6A). In the presence of more than fourfold molar excess amounts of nucleobase, **pPyNFP** exhibited a hyperchromic spectral change without a shift of λ_{max} (S-II was 495 nm) (Fig. 6B). This spectral change was closely similar to that seen in the presence of long dsDNA.

We finally addressed the importance of the polymer structure of DNA by examining the effect of deoxyribonucleotide triphosphate (dNTP, an equivalent mixture of dATP, dGTP, dCTP and dTTP). The addition of dNTP caused a modest hyperchromic change without a red-shift (Fig. 7). This result suggests that dNTP modestly resolves aggregation of **pPyNFP**, but gives no significant electronic perturbation to the NFP macrocycle. Under the same conditions, **pPyP** only showed a very small spectral change upon the addition of dNTP (Fig. S4†).

Interactions of pPyNFP with G-quadruplex DNAs

G-quadruplex DNA structures, which are formed in the presence of K^+ or Na^+, have been considered to play pivotal roles in gene expression and DNA replication.[35–38] Their biological importance makes G-quadruplex DNA structures attractive targets for DNA-binding ligands of small size[39–44] and some ligands have been the subject of *in vivo* anticancer studies.[45–47] We have examined the interactions between **pPyNFP** and G-quadruplex DNAs derived from human telomere sequence.

We first investigated the ability of **pPyNFP** to stabilize a K^+-induced G-quadruplex structure using the G4 DNA (5′-CATGGTGG-TTTGGG-$(TTAGGG)_3$-ACCAC-3′), which has been used frequently for CD thermal melting experiments.[48,49] In the presence of K^+, G4 DNA exhibited a CD signal that is characteristic of a mixed (3 + 1) parallel/antiparallel structure[50] and is not influenced by **pPyNFP** (Fig. S5A†). In the presence of 100 mM K^+ ions, the melting temperature (T_m) of G4 DNA increased with an increase in the concentration of **pPyNFP**, indicating that **pPyNFP** stabilizes a (3 + 1) parallel/antiparallel G-quadruplex structure (Table 1, see also Fig. S5B†). A comparative measurement of the CD melting curves with **pPyP** indicates that the extent of stabilization of the G-quadruplex structure by **pPyNFP** was nearly same as that by **pPyP** (Table 1, see also Fig. S5C†).

Recently small molecules with an ability to modulate G-quadruplex structures of the human telomeric sequence have been attracting considerable attention because they may be applicable

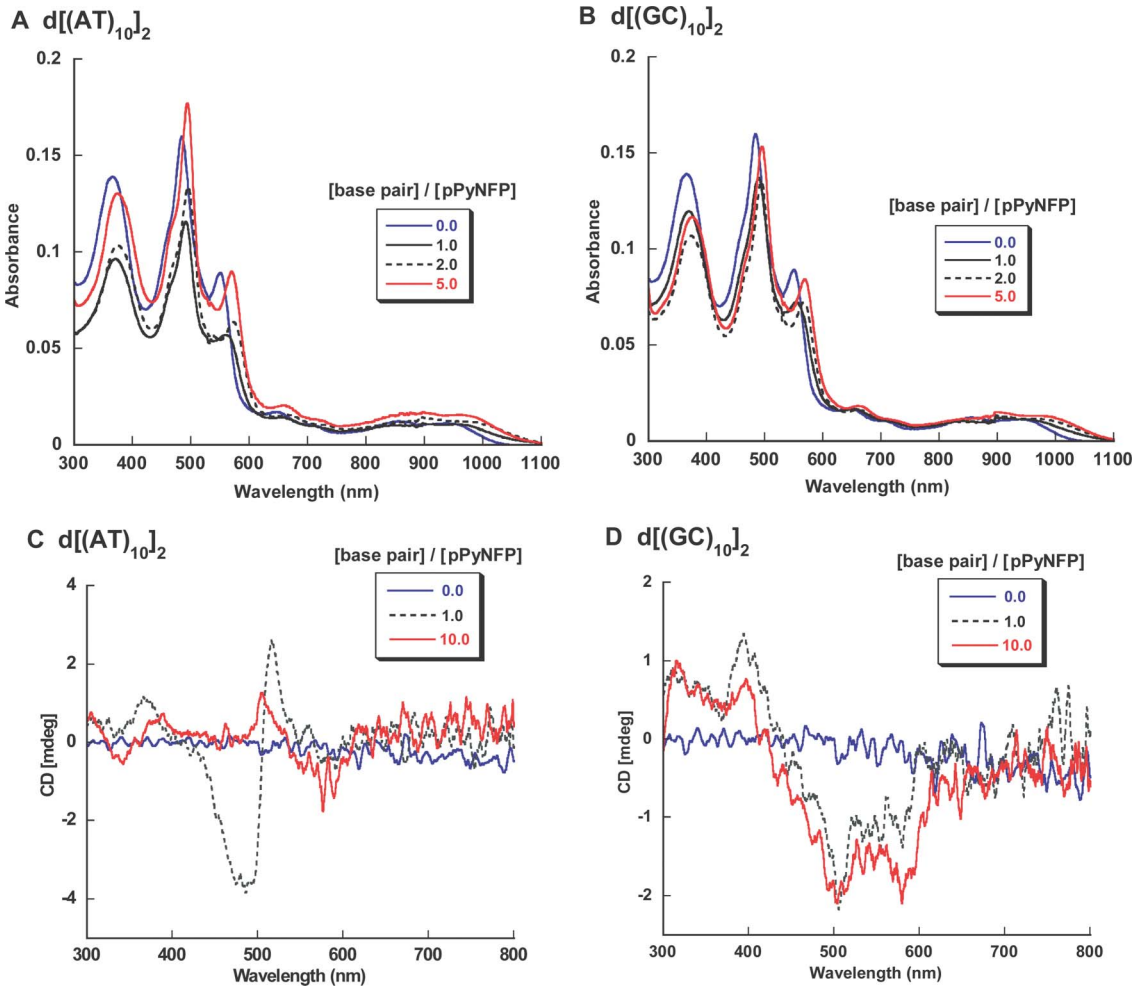

Fig. 5 The interactions of **pPyNFP** with A:T and G:C base pairs. A, B: UV-vis–NIR absorption spectra of **pPyNFP** (7.5 μM) in the presence of A:T (A) or G:C (B) base pairs at pH 7.0 with 50 mM HEPES. C, D: Circular dichroism (CD) spectra of **pPyNFP** (7.5 μM) in the presence of A:T (C) or G:C (D) base pairs at pH 7.0 with 50 mM HEPES.

Table 1 CD melting temperatures of G4 DNA in the presence of different concentrations of **pPyNFP** and **pPyP**

Compound		r = [compound]/[G4 DNA]			
		0 (DNA alone)	1	3	5
pPyNFP					
	T_m (°C)	51.7 ± 0.6	54.3 ± 0.4	58.0 ± 0.4	60.7 ± 0.5
	ΔT_m (°C)	---	2.6 ± 0.2	6.3 ± 0.2	9.0 ± 0.1
pPyP	T_m (°C)	51.7 ± 0.6	55.6 ± 0.8	58.5± 0.4	61.1 ± 0.3
	ΔT_m (°C)	---	3.9 ± 0.2	6.8 ± 0.2	9.4 ± 0.4

to the regulation of telomerase activity.[51–56] The human telomeric sequence (5′-(TTAGGG)$_4$-3′ abbreviated as (T$_2$AG$_3$)$_4$) adapts several types of G-quadruplex structures depending on the state of the DNAs (in crystals or in solution) and monovalent metal ions (Scheme S1†).[50,57–60] In solution, (T$_2$AG$_3$)$_4$ DNA forms a highly stable (3 + 1) parallel/antiparallel structure with K^+ (Scheme S1A†)[50,57] and it also forms a (2 + 2) antiparallel structure with Na^+ (Scheme S1B†).[58] The two types of G-quadruplexes exhibited different CD signals.[49] We investigated whether **pPyNFP** is capable of inducing a structural change of G-quadruplex structures of (T$_2$AG$_3$)$_4$ DNA.

In the presence of K^+ ions, which induce the highly stable (3 + 1) parallel/antiparallel structure, the CD signal of (T$_2$AG$_3$)$_4$ DNA was unaffected by the addition of **pPyNFP** (Fig. 8A). This result is consistent with the observation that **pPyNFP** stabilizes the K^+-induced G-quadruplex of G4 DNA (Fig. S5A†). We then tested the (2 + 2) antiparallel structure induced by Na^+ (Fig. 8B). Upon the addition of **pPyNFP**, the characteristic CD signal of the (2 + 2) antiparallel structure (a positive peak at around 245 nm and negative peak at around 265 nm) diminished and the CD signal showed a weak negative peak at around 240 nm and a positive peak at around 270 nm (Fig. 8B). The CD thermal melting profile showed that T_m of the (T$_2$AG$_3$)$_4$ DNA structure with 100 mM Na^+ increased (+7.6 °C) upon the addition of 5 molar equivalent of **pPyNFP** (Fig. S5D, Table S1†), indicating that the DNA structure associated with **pPyNFP** was more stable than the initial (2 + 2) antiparallel structure induced by Na^+.

Since the CD spectra induced by **pPyNFP** was distinct from those induced by K^+ and Na^+, the resulting structure with **pPyNFP** may be different from the (3 + 1) parallel/antiparallel and (2 + 2) antiparallel structures. The CD spectra induced by **pPyNFP**, which exhibited a weak negative peak at around 240–250 nm and a positive peak at around 270 nm, share features with the CD

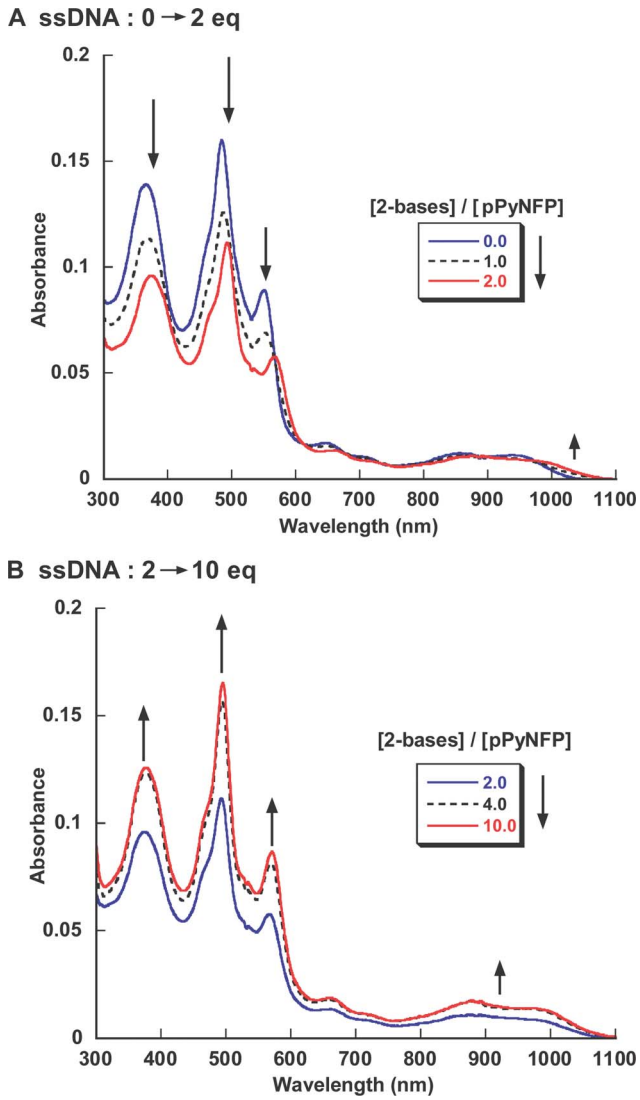

Fig. 6 The single stranded DNA (ssDNA) binding ability of **pPyNFP**. UV-vis–NIR absorption spectra of **pPyNFP** (7.5 μM) in the presence of less (A) or more (B) than 1 equivalent molar amounts of ssDNA base at pH 7.0 with 50 mM HEPES.

signals of parallel-type G-quadruplex structures that also exhibit a weak negative peak at around 240 nm and a positive peak at around 260–270 nm.[35,36] No similar change was observed upon the addition of **pPyP** (Fig. S6†). Although further analyses are needed, the CD analyses in this study suggest that **pPyNFP** interacts with $(T_2AG_3)_4$ DNA and can induce a parallel G-quadruplex structure in the absence of K^+. This possibility is also supported by the fact that $(T_2AG_3)_4$ DNA forms a parallel G-quadruplex structure in the single crystal state (Scheme S1C†). In the absence of monovalent metal ions, **pPyNFP** also induced a CD signal from DNA (Fig. S7A†), which was similar to that in the presence of Na^+.

We are also interested in the influence of the stable (3 + 1) parallel/antiparallel DNA structure on the aggregation property of **pPyNFP**. In the absence of K^+ ions, the effect of G4 DNA on **pPyNFP** was closely similar to that observed with unstructured ssDNA (Fig. S7B†). In the presence of 100 mM K^+ ions, however, the effects of $(T_2AG_3)_4$ DNA on **pPyNFP** were different from those of ss- and ds-DNAs. In the presence of less than 12

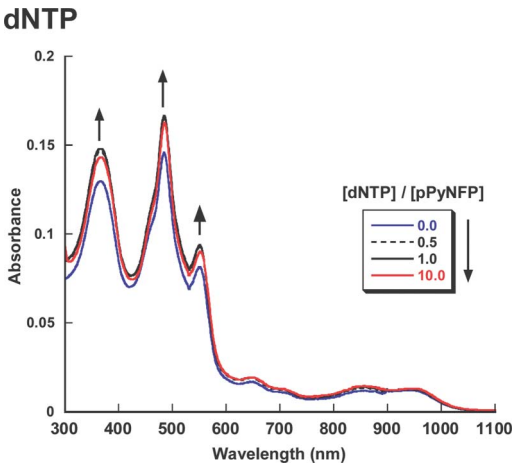

Fig. 7 The effects of deoxyribonucleotide triphosphate on **pPyNFP**. UV-vis–NIR absorption spectra of **pPyNFP** (7.5 μM) in the presence of deoxyribonucleotide triphosphate (dNTP) at pH 7.0 with 50 mM HEPES.

equimolar amounts of DNA bases (0.5 equimolar amounts of the G-quadruplex structure), a hyperchromic effect was observed (Fig. 9A), suggesting that **pPyNFP** formed a sparse aggregate. In the presence of more than 0.5 equimolar amounts of the G-quadruplex structure, a hypochromic spectral change was observed (Fig. 9B), suggesting that **pPyNFP** received electronic perturbation caused by π–π stacking interactions. Although the determination of the accurate association constants (K_a) of **pPyNFP** for $(T_2AG_3)_4$ DNA is difficult due to the complex spectral change (Figs 9 and S8†), we preliminarily estimated K_a's from the spectral change of **pPyNFP** with more than 12 equimolar amounts of DNA bases (Figs 9B and S8B†).[61] The roughly estimated K_a values are 5.6×10^6 M^{-1} and 1.7×10^7 M^{-1} in the presence of K^+ and Na^+ respectively. These values seem comparable to those of **pPyP** (2.4×10^7 M^{-1}) and **pPyNCP** (5.3×10^6 M^{-1}) for the K^+-induced G-quadruplex formed by the human telomeric DNA sequence.[49]

In the presence of more than 12 equimolar amounts of DNA bases (0.5 equimolar amounts of the G-quadruplex structure), **pPyNFP** exhibited induced CD signals (Fig. 9C) that were different from those induced by double stranded DNAs. These observations indicated that the dose-dependent effects of the stable G-quadruplex DNA on **pPyNFP** were different from those of ss- and dsDNA.

Although the molecular mechanism causing such a difference is not clear, higher order structures of G-quadruplex DNA might be involved in this spectral change.[60,62–63] For instance, G-quadruplex DNAs could form an oligomeric structure, in which three G-quintets form a structural unit (G4 unit) and a TTA serves as a linker to connect two G4 units. Since the TTA linker region provides a molecular cleft (Scheme S2A†), a possible model is that **pPyNFP** could be captured in the cleft between the G4 unit, in which the NFP skeleton was sandwiched by two G-quintets flanked by the TTA linker. Alternatively, **pPyNFP** has an ability to assemble the monomeric G-quadruplex structure without oligomer formation (Scheme S2B†).

Conclusions

We have synthesized a water-soluble derivative of N-fused porphyrin bearing cationic side-arms (**pPyNFP**) and elucidated

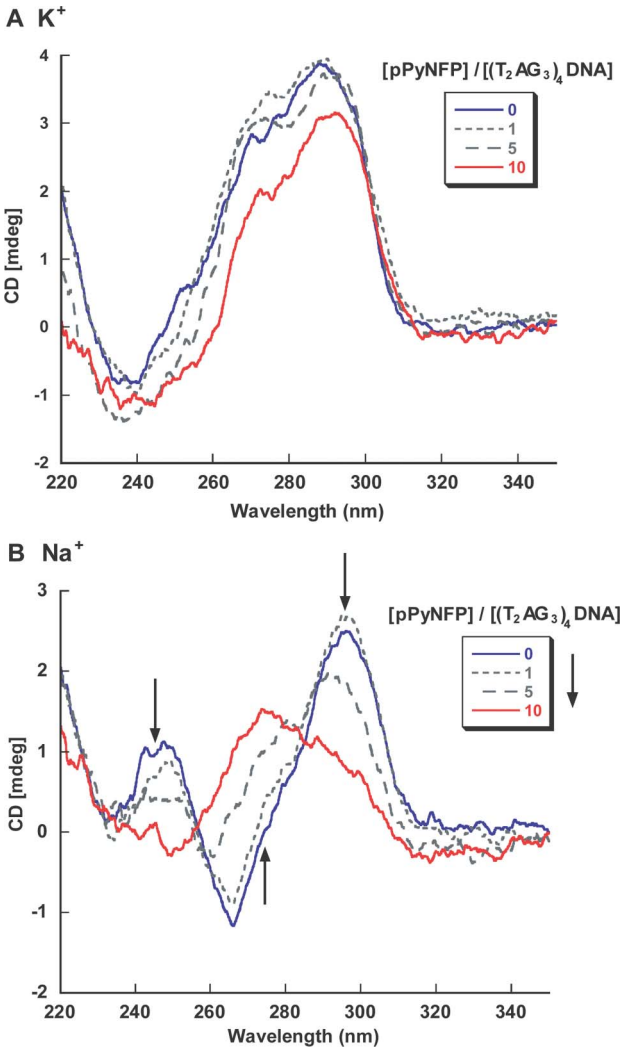

Fig. 8 The effects of **pPyNFP** on different G-quadruplex DNA structures. A: CD titration of $(T_2AG_3)_4$ DNA with the (3 + 1) parallel/antiparallel structure induced by 100 mM K^+ ions with 10 mM Tris-HCl (pH 7.4) and 1 mM EDTA. B: CD titration of $(T_2AG_3)_4$ DNA with the (2 + 2) antiparallel structure induced by 100 mM Na^+ ions with 10 mM Tris-HCl (pH 7.4) and 1 mM EDTA.

its acid–base and DNA-binding properties. From pH titration experiments, **pPyNFP** accepts two protons in a stepwise manner. UV-vis–NIR and induced-CD spectral changes upon the additions of DNAs revealed that **pPyNFP** can bind to ss- and dsDNA. In the titration of **pPyNFP** with a long dsDNA, clear spectral changes were observed with 0.4 equimolar amounts of DNA base pairs. Under the same conditions, **pPyP** showed only a small spectral change with 0.5 equimolar amounts of DNA base pairs, suggesting that the binding affinity of **pPyNFP** to dsDNA is even better than **pPyP**. This observation indicates that the NFP skeleton is a promising platform to develop high-affinity DNA binding molecules.

The induced CD spectra of DNA strongly suggest that **pPyNFP** can induce a structural change of $(T_2AG_3)_4$ DNA to an all-parallel structure. In contrast, such a structural change was not induced by **pPyP**. Recently, it was also reported that **pPyNCP** induces a structural change of $(T_2AG_3)_4$ DNA to a (3 + 1)

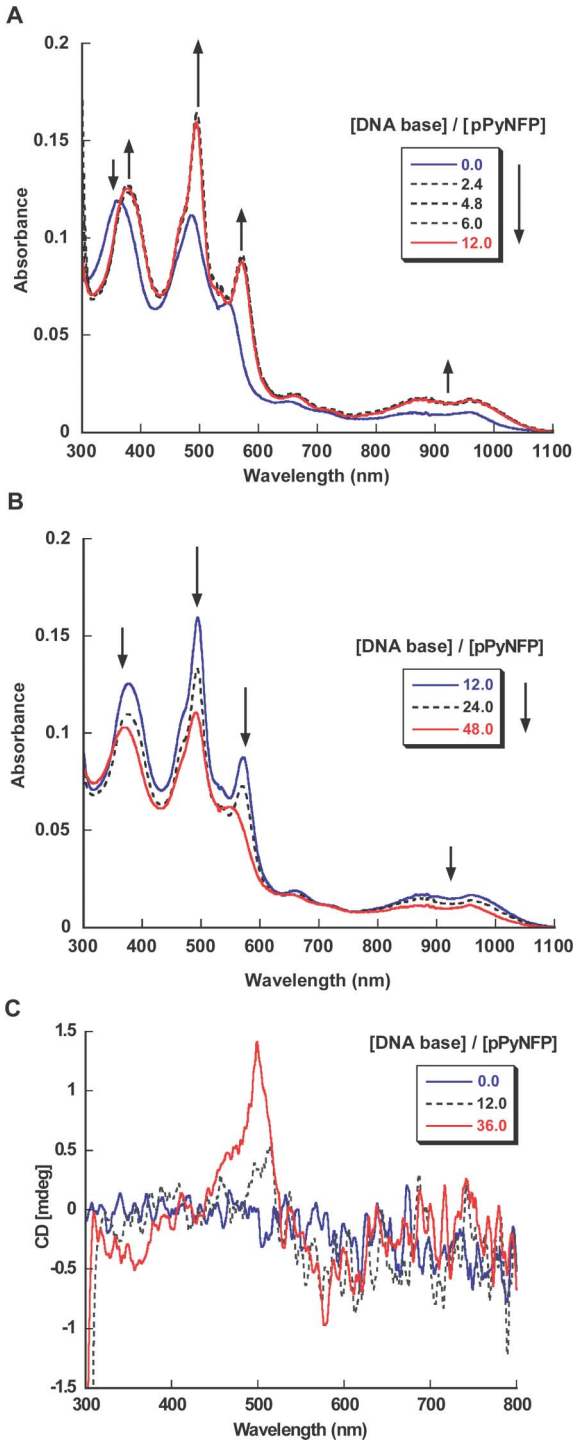

Fig. 9 Effects of the stable G-quadruplex DNA structure on the absorption property of **pPyNFP**. A, B: UV-vis–NIR absorption spectra of **pPyNFP** (7.5 μM) in the presence of less (A) or more (B) than a 0.5 equivalent molar amount of the stable (3 + 1) parallel/antiparallel structure induced by 100 mM K^+ ions with 10 mM Tris-HCl (pH 7.4) and 1 mM EDTA. C: Circular dichroism (CD) spectra of **pPyNFP** (7.5 μM) in the presence of the stable (3 + 1) parallel/antiparallel structure induced by 100 mM K^+ ions with 10 mM Tris–HCl (pH 7.4) and 1 mM EDTA.

parallel/antiparallel structure. These observations indicate that the structural variation of tetrapyrrolic macrocycles (regular, N-fused, and N-confused porphyrins) gives distinct effects on

$(T_2AG_3)_4$ DNA, even though they possess the same pyridinium side-arms.

The present study also demonstrated that **pPyNFP** binds with G-quadruplex DNA with an affinity comparable to that between **pPyP** and G-quadruplex DNA. Since small molecules recognizing the higher order structures of G-quadruplexes are of significant interest,[63] a comprehensive study of the interactions between oligomeric G-quadruplexes and water-soluble porphyrinoids is in progress. This study also implicates that the porphyrin-related macrocycles would be a promising toolbox for modulating the G-quadruplex DNAs and also their higher order structures. In addition, a nucleophile-induced skeletal rearrangement of NFP to NCP has been reported.[22] As such, skeletal conversion has never been achieved by regular porphyrins and it is attractive to apply this characteristic property to stimulus-induced regulation of G-quadruplex structures.

Experimental Section

Chemicals

For chemical synthesis, commercially available reagents and solvents were used without further purification. Silica gel column chromatography was performed on KANTO Silica Gel 60 N (spherical, neutral, particle size 40–50 μm). For preparation of aqueous buffer solutions for optical measurements, molecular biology grade reagents (Nacalai Tesque, Kyoto, Japan) and ultrapure water (prepared by Organo Puric-Z, Tokyo, Japan) were employed. Double stranded DNA (dsDNA) from salmon testes was purchased from Sigma-Aldrich Japan (Tokyo, Japan). Synthetic DNAs, which are ssDNA (5′-TGTAGGCATGCTTAAGCAT-3′), $d(AT)_{10}$ (5′-ATATATATATATATATATAT-3′), and $d(GC)_{10}$ (5′-GCGCGCGCGCGCGCGCGC-3′), were purchased from Hokkaido System Science (Hokkaido, Japan). G4 DNA (5′-CATGGTGG-TTTGGG- $(TTAGGG)_3$-ACCAC-3′) and $(T_2AG_3)_4$ DNA (5′-$(TTAGGG)_4$-3′) were purchased from Sigma-Aldrich Japan (Tokyo, Japan). Concentrations of the DNA solutions were calculated from the absorbance at 260 nm. In the DNA titration experiments, the molar ratios between the compounds and DNA were adjusted using the molar concentrations of DNA base pairs for dsDNA, $[d(AT)_{10}]_2$ and $[d(GC)_{10}]_2$, or with those of nucleobases for ssDNA, G4 DNA and $(T_2AG_3)_4$ DNA, respectively.

Spectral measurements

^{1}H NMR spectra were recorded on a JEOL JNM-AL300 spectrometer (operating 300.40 MHz for ^{1}H). Chemical shifts were expressed in parts per million from a residual portion of deuterated solvent, $CHCl_3$ (δ = 7.26), DMSO (δ = 2.50). UV-vis–NIR spectra were measured using 10 mm quartz cells at ambient temperature and spectra were recorded on a Shimadzu UV-3150PC spectrometer. CD spectra were recorded on a JASCO J-720 spectropolarimeter equipped with a PTC-423 L temperature controller using a quartz cell with an optical path length of 2 mm in a reaction volume of 600 μL and an instrument scanning speed of 100 nm min^{-1}, a 0.5 nm pitch and a 1 nm bandwidth, with a response time of 2 s over a wavelength range of 220–350 nm. The scan of the buffer was subtracted from the average scan for each sample. CD spectra were collected in units of molar circular dichroism *versus* wavelength. The cell holding chamber was flushed with a constant stream of dry nitrogen gas to prevent the condensation of water on the cell exterior. All of the DNA samples were dissolved and diluted in suitable buffers containing appropriate concentrations of ions. DNA samples were annealed at 95–98 °C for 5 min and then allowed to cool for 2 h to the initial temperature at which the samples were kept at the beginning of the experiment. The CD data represent three averaged scans taken over a temperature range 20–95 °C. All CD spectra are baseline-corrected for signal contributions caused by the buffer. The CD melting profiles were recorded at 295 nm. The temperature ranged 20–99 °C and the heating rate was 1.0 °C min^{-1}. The melting temperature (T_m) was defined as the temperature of the mid-transition point.

Synthesis

5,10,15,20-Tetrakis(*p*-(methoxymethoxy)methyl)phenyl)-2-aza-21-carbaporphyrin (1). To a solution of pyrrole (2.081 mL, 30.0 mmol) and 4-methoxymethoxymethyl benzaldehyde (5.406 g, 30.0 mmol) in CH_2Cl_2 (3.0 L) at room temperature, methanesulfonic acid (1.363 mL, 21 mmol) was added. The mixture was stirred at room temperature for 30 min. Then, 2,3-dichloro-5,6-dicyano-*p*-benzoquinone (DDQ) (5.99 g, 26.4 mmol) was added. After 1 min, triethylamine (11.7 mL, 84.0 mmol) was added. The reaction mixture was separated by column chromatography on a silica gel with CH_2Cl_2 as the eluent. The second dark yellow–green fraction gave NCP **1** (1534.5 mg, 1.576 mmol) in 21% yield. ^{1}H NMR ($CDCl_3$): δ –5.04 (s, 1H, inner CH), 3.54 (s, 3H, -OCH_3), 3.55 (s, 3H, –OCH_3), 3.57 (s, 6H, -OCH_3), 4.90–4.93 (m, 16H, –OCH_2OCH_2-), 7.73 (d, J = 6.3 Hz, 4H, Ph), 7.82 (d, J = 7.8 Hz, 2H, Ph), 7.83 (d, J = 7.8 Hz, 2H, Ph), 8.11–8.15 (m, 4H, Ph), 8.31 (d, J = 7.8 Hz, 2H, Ph), 8.35 (d, J = 7.8 Hz, 2H, Ph), 8.53–8.57 (m, 3H, β-pyrrole), 8.59 (d, J = 5.1 Hz, 1H, β-pyrrole), 8.73 (s, 1H, outer α-pyrrole), 8.91 (d, J = 5.1 Hz, 1H, β-pyrrole), 8.96 (d, J = 4.8 Hz, 2H, β-pyrrole); MS (MALDI): m/z 910.39; UV-vis–NIR (CH_2Cl_2, λ_{max} nm^{-1}): 440.0, 542.5, 584.0, 728.5.

N-Fused 5,10,15,20-tetrakis(*p*-(methoxymethoxy)methyl)phenyl)porphyrin (4). To a CH_2Cl_2 solution of NCP **1** (2.0 g, 2.195 mmol), NBS (899.0 mg, 5.05 mmol) was added and the resulting solution was stirred for 10 min. The reaction mixture was separated on a silica gel column with CH_2Cl_2. The second green fraction gave dibrominated NCP **2** (1.60 g, 1.50 mmol) in 68.2% yield. Then, a pyridine solution of **2** (1558 mg, 1.46 mmol) was stirred for 12 h at ambient temperature. After evaporation, the residues were separated by chromatography on a silica gel column with CH_2Cl_2 as eluent. The third red fraction gave monobrominated NFP **3** (772.0 mg, 0.781) in 54% yield. As the fourth fraction, NFP **4** (115 mg, 0.127 mmol) was obtained in 8.7% yield. A pyridine solution of monobrominated NFP **3** (772 mg, 0.781 mmol) was refluxed for 12 h. After evaporation, the residue was separated by chromatography on a silica gel column with CH_2Cl_2 as the eluent. The third red fraction recovered unreacted **3** (317 mg, 0.318 mmol, 41%), and the fourth red fraction gave NFP **4** (34 mg, 0.037 mmol) in 4.8% yield. ^{1}H NMR ($CDCl_3$): δ 3.51–3.60 (m, 12H), 4.78–4.95 (m, 16H), 7.62 (d, 1H, J = 4.8 Hz), 7.65–7.78 (m, 7H), 7.85 (d, 1H, J = 4.8 Hz), 7.95–8.00

(m, 3H), 8.05–8.10 (m, 5H), 8.40 (d, 2H, J = 6.1 Hz), 8.61 (d, 1H, 5.4 Hz), 8.74 (d, 2H, J = 8.4 Hz), 9.11 (d, 1H, J = 4.8 Hz), 9.30 (s, 1H); MS (MALDI): m/z 908.38; UV-vis-NIR (CH_2Cl_2, λ_{max} nm^{-1}): 361.5, 500.0, 548.5, 650.5, 706.0, 860.0, 943.0.

N-Fused 5,10,15,20-tetrakis(*p*-(hydroxymethyl)phenyl)porphyrin (5). A trifluoroacetic acid (TFA) (5 mL) solution of **4** (107 mg, 0.146 mmol) was stirred for few minutes. Then, H_2O (5 mL) was added and the solution was sealed with a glass cap and stirred for 3 days. The reaction mixture was washed with aq. $NaHCO_3$ solution and the precipitated product was filtrated. The obtained solid was purified with chromatography over a silica gel column (THF: Hexane = 5: 1) to afford **5** in 71% yield (75.8 mg, 0.103 mmol). ^{1}H NMR (DMSO-d_6): δ 4.70–4.87 (m, 8H), 5.25–5.50 (m, 4H), 7.47 (d, 1H, J = 5.1 Hz), 7.60–7.75 (m, 6H), 7.89 (d, 2H, J = 7.8 Hz), 7.94 (d, 2H, J = 7.8 Hz), 7.95–8.01 (m, 4H), 8.12 (d, 1H, J = 4.8 Hz), 8.24 (d, 2H, J = 7.8 Hz), 8.50 (d, 1H, J = 4.8 Hz), 8.63 (s, 1H), 8.84 (d, 2H, J = 8.4 Hz), 9.29 (s, 1H), 9.56 (d, 1H, J = 5.4 Hz); MS (MALDI): m/z 732.82; UV-vis–NIR (DMSO, λ_{max}/nm): 367.0, 500.5 550.5, 649.5, 705.5, 864.5, 951.0.

N-Fused 5,10,15,20-tetrakis(α-pyridinio-*p*-tolyl)porphyrin tetratrifluoroacetate salt (pPyNFP · 4CF_3COO^-). To a pyridine (1.0 mL) solution of **5** (5 mg, 0.0068 mmol) was added a pyridine solution (0.5 mL) of methanesulfonyl chloride (10.6 μL, 0.136 mmol) to yield a tetramesylate derivative **6**, which was further converted to **pPyNFP** in the solution. The resulting solution was stirred for 3 h at room temperature. The reaction mixture was filtrated and washed with pyridine and dichloromethane. Crude **pPyNFP** tetramethanesulfonate salt was dissolved in ultra-pure water and purified by HPLC with CosmoSil 5C18-AR-II (4.6 × 250 mm) using a mixed solvent CH_3CN/H_2O containing 0.1% TFA. Gradient conditions for CH_3CN in 0.1% aq TFA were as follows: 0–50% in 30 min. The flow rate was 1 mL min^{-1} and the absorption at 550 nm was employed for detection of the NFP moiety. The desired fraction was collected and lyophilized to afford tetratrifluoroacetate salt of the target compound **pPyNFP** as a dark-red solid. ^{1}H NMR (DMSO-d_6): δ 6.11–6.28 (m, 8H), 7.61 (s, 1H), 7.77–8.01 (m, 8H), 8.03–8.12 (m, 4H), 8.19 (d, 3H, J = 7.8 Hz), 8.23–8.40 (m, 9H), 8.55 (d, 2H, J = 8.1 Hz), 8.64 (d, 1H, J = 4.8 Hz), 8.68–8.82 (m, 4H), 9.02 (d, 2H, J = 8.1 Hz), 9.40 (t, 4H), 9.48 (d, 4H, J = 6.6 Hz), 9.64 (s, 1H), 9.76 (s, 1H); HRMS (ESI$^+$): m/z; found: 245.103, calcd for $C_{64}H_{52}N_8$ (MH^+)/4: 245.107; UV-vis–NIR (DMSO, λ_{max}/nm): 367.5, 502.5 550.5, 652.0, 708.0, 857.0, 942.0.

Acknowledgements

We acknowledge Drs. Atsushi Maruyama and Naohiko Shimada for the help with measurements of the CD spectra. This work is supported by Grants-in-Aids for Challenging Exploratory Research (No.23655159 to Y.I.), on Innovative Areas "Emergence in Chemistry" (No.21111518 to Y.I.) and "Emergence of highly elaborated π-space and its function" (No. 21108518 to H.F.) and also by the Global COE Program "Science for Future Molecular Systems" (H.F.) from the Ministry of Education, Culture, Sports, Science and Technology (MEXT), Japan.

References

1 K. M. Kadish, K. M. Smith and R. Guilard, *Handbook of Porphyrin Science*, World Scientific: Singapore, 2010, Vol. 1–15.
2 R. J. Fiel, J. C. Howard, E. H. Mark and N. Datta-Gupta, *Nucleic Acids Res.*, 1979, **6**, 3093–3118.
3 R. J. Fiel, *J. Biomol. Struct. Dyn.*, 1989, **6**, 1259–1274.
4 P. Kubát, K. Lang, P. Anzenbacher Jr., K. Jursíková, V. Král and B. Ehrenberg, *J. Chem. Soc. Perkin Trans. 1*, 2000, 933–941.
5 D. R. McMillin, A. H. Shelton, S. A. Bejune, P. E. Fanwick and R. K. Wall, *Coord. Chem. Rev.*, 2005, **249**, 1451–1459.
6 C. Romera, L. Sabater, A. Garofalo, I. M. Dixon and G. Pratviel, *Inorg. Chem.*, 2010, **49**, 8558–8567.
7 L. G. Marzilli, *New J. Chem.*, 1990, **14**, 409–420.
8 Y. H. Chae, B. Jin, J. K. Kim, S. W. Han, S. K. Kim and H. M. Lee, *Bull. Korean Chem. Soc.*, 2007, **28**, 2203–2208.
9 J. Seenisamy, S. Bashyam, V. Gokhale, H. Vankayalapati, D. Sun, A. Siddiqui-Jain, N. Streiner, K. Shin-Ya, E. White, W. D. Wilson and L. H. Hurley, *J. Am. Chem. Soc.*, 2005, **127**, 2944–2959.
10 Z. Gershman, I. Goldberg and Z. Gross, *Angew. Chem., Int. Ed.*, 2007, **46**, 4320–4324.
11 A. K. Bordbar, M. Davari, E. Safaei and V. Mirkhani, *J. Porphyrins Phthalocyanines*, 2007, **11**, 139–147.
12 Y. Ikawa, S. Moriyama, H. Harada and H. Furuta, *Org. Biomol. Chem.*, 2008, **6**, 4157–4166.
13 X. Ragàs, D. Sánchez-García, R. Ruiz-González, T. Dai, M. Agut, M. R. Hamblin and S. Nonell, *J. Med. Chem.*, 2010, **53**, 7796–7803.
14 J. L. Sessler and S. J. Weghorn, *Expanded Contracted & Isomeric Porphyrins*, Elsevier, Oxford, 1997.
15 P. J. Chmielewski and L. Latos-Grażyński, *Coord. Chem. Rev.*, 2005, **249**, 2510–2533.
16 I. Gupta and M. Ravikanth, *Coord. Chem. Rev.*, 2006, **250**, 468–518.
17 R. Misra and T. K. Chandrashekar, *Acc. Chem. Res.*, 2008, **41**, 265–279.
18 Y. Inokuma and A. Osuka, *Dalton Trans.*, 2008, 2517–2526.
19 D. Sanchez-Garcia and J. L. Sessler, *Chem. Soc. Rev.*, 2008, **37**, 215–232.
20 J. Y. Shin, K. S. Kim, M. C. Yoon, J. M. Lim, Z. S. Yoon, A. Osuka and D. Kim, *Chem. Soc. Rev.*, 2010, **39**, 2751–2767.
21 H. Furuta, T. Ishizuka, A. Osuka and T. T. Ogawa, *J. Am. Chem. Soc.*, 1999, **121**, 2945–2946.
22 H. Furuta, T. Ishizuka, A. Osuka and T. Ogawa, *J. Am. Chem. Soc.*, 2000, **122**, 5748–5757.
23 T. Ishizuka, S. Ikeda, M. Toganoh, I. Yoshida, Y. Ishikawa, A. Osuka and H. Furuta, *Tetrahedron*, 2008, **64**, 4037–4050.
24 M. Toganoh, T. Kimura, H. Uno and H. H. Furuta, *Angew. Chem., Int. Ed.*, 2008, **47**, 8913–8916.
25 Y. Ikawa, H. Harada, M. Toganoh and H. Furuta, *Bioorg. Med. Chem Lett.*, 2009, **19**, 2448–2452.
26 S. Ikeda, M. Toganoh, S. Easwaramoorthi, J. M. Lim, D. Kim and H. Furuta, *J. Org. Chem.*, 2010, **75**, 8637–8649.
27 P. Hambright in *The Porphyrin Handbook*, ed. K. M. Kadish, K. M. Smith and R. Guilard, Academic Press, California, 2000, Chapter 18.
28 S. Thyagarajan, T. Leiding, S. P. Arsköld, A. V. Cheprakov and S. A. Vinogradov, *Inorg. Chem.*, 2010, **49**, 9909–9920.
29 T. Weitner, A. Budimir, I. Kos, I. Batinić-Haberle and M. Biruš, *Dalton Trans.*, 2010, **39**, 11568–11576.
30 Y. Ikawa, H. Ogawa, H. Harada and H. Furuta, *Bioorg. Med. Chem. Lett.*, 2008, **18**, 6394–6397.
31 N. E. Mukundan, G. Petho, D. W. Dixon, M.-S. Kim and L. G. Marzilli, *Inorg. Chem.*, 1994, **33**, 4676–4687.
32 K. S. Dancil, L. F. Hilario, R. G. Khoury, K. U. Mai, C. K. Nguyen, K. S. Weddle and A. M. Shachter, *J. Heterocyclic. Chem.*, 1997, **34**, 749–755.
33 N. C. Maiti, M. Mazumdar and N. Periasamy, *J. Phys. Chem. B*, 1998, **102**, 1528–1538.
34 S. C. M. Gandini, I. E. Borissevitch, J. R. Perussi, H. Imasato and M. Tabak, *J. Lumin.*, 1998, **78**, 53–61.
35 J. R. Williamson, *Curr. Opn. Struct. Biol.*, 1993, **3**, 357–362.
36 S. Burge, G. N. Parkinson, P. Hazel, A. K. Todd and S. Neidle, *Nucleic Acids Res.*, 2006, **34**, 5402–5415.
37 H. J. Lipps and D. Rhodes, *Trends Cell. Biol.*, 2009, **19**, 414–422.
38 J. L. Huppert, *FEBS J.*, 2010, **277**, 3452–3458.
39 T. M. Ou, Y. J. Lu, J. H. Tan, Z. S. Huang, K. Y. Wong and L. Q. Gu, *ChemMedChem*, 2008, **3**, 690–713.
40 D. Monchaud, A. Granzhan, N. Saettel, A. Guédin, J. L. Mergny and M. P. Teulade-Fichou, *J. Nucleic Acids.*, 2010, 525862.

41 M. C. Nielsen and T. Ulven, *Curr. Med. Chem.*, 2010, **17**, 3438–3448.
42 S. Balasubramanian and S. Neidle, *Curr. Opin. Chem. Biol.*, 2009, **13**, 345–353.
43 Y. Xu, *Chem. Soc. Rev.*, 2011, **40**, 2719–27140.
44 D. J. Patel, A. T. Phan and V. Kuryavyi, *Nucleic Acids Res.*, 2007, **35**, 7429–7455.
45 A. M. Burger, F. Dai, C. M. Schultes, A. P. Reszka, M. J. Moore, J. A. Double and S. Neidle, *Cancer Res.*, 2005, **65**, 1489–1496.
46 P. Phatak, J. C. Cookson, F. Dai, V. Smith, R. B. Gartenhaus, M. F. Stevens and A. M. Burger, *Br. J. Cancer.*, 2007, **96**, 1223–1233.
47 T. Tauchi, K. Shin-ya, G. Sashida, M. Sumi, S. Okabe, J. H. Ohyashiki and K. Ohyashiki, *Oncogene*, 2006, **25**, 5719–5725.
48 T. Yamashita, T. Uno and Y. Ishikawa, *Bioorg. Med. Chem.*, 2005, **13**, 2423–2430.
49 Y. Du, D. Zhang, W. Chen, M. Zhang, Y. Zhou and X. Zhou, *Bioorg. Med. Chem.*, 2010, **18**, 1111–1116.
50 A. Ambrus, D. Chen, J. Dai, T. Bialis, R. A. Jones and D. Yang, *Nucleic Acids Res.*, 2006, **34**, 2723–2735.
51 K. Nakatani, S. Hagihara, S. Sando, S. Sakamoto, K. Yamaguchi, C. Maesawa and I. Saito, *J. Am. Chem. Soc.*, 2003, **125**, 662–666.
52 D. P. Gonçalves, R. Rodriguez, S. Balasubramanian and J. K. Sanders, *Chem. Commun.*, 2006, 4685–4687.
53 D. P. Gonçalves, S. Ladame, S. Balasubramanian and J. K. Sanders, *Org. Biomol. Chem.*, 2006, **4**, 3337–3342.
54 B. Fu, J. Huang, L. Ren, X. Weng, Y. Zhou, Y. Du, X. Wu, X. Zhou and G. Yang, *Chem. Commun.*, 2007, 3264–3266.
55 S. Yang, J. Xiang, Q. Yang, Q. Zhou, X. Zhang, Q. Li, Y. Tang and G. Xu, *Fitoterapia*, 2010, **81**, 1026–1032.
56 S. K. Pradhan, D. Dasgupta and G. Basu, *Biochem. Biophys. Res. Comm.*, 2011, **404**, 139–142.
57 Y. Xu, Y. Noguchi and H. Sugiyama, *Bioorg. Med. Chem.*, 2006, **14**, 5584–5591.
58 Y. Wang and D. J. Patel, *Structure*, 1993, **15**, 263–282.
59 G. N. Parkinson, M. P. Lee and S. Neidle, *Nature*, 2002, **417**, 876–880.
60 D. Sen and W. Gilbert, *Biochemistry*, 1992, **31**, 65–70.
61 H. Mita, T. Ohyama, Y. Tanaka and Y. Yamamoto, *Biochemistry*, 2006, **45**, 6765–6772.
62 H.-Q. Yu, D. Miyoshi and N. Sugimoto, *J. Am. Chem. Soc.*, 2006, **128**, 15461–15468.
63 K. Shinohara, Y. Sannohe, S. Kaieda, K. Tanaka, H. Osuga, H. Tahara, Y. Xu, T. Kawase, T. Bando and H. Sugiyama, *J. Am. Chem. Soc.*, 2010, **132**, 3778–3782.

